Engineering Structures 196 (2019) 109277

Contents lists available at ScienceDirect

Engineering Structures

journal homepage: www.elsevier.com/locate/engstruct

Design of steel bridge girders against ship forecastle collisions

Yanyan Sha[a,c,*], Jørgen Amdahl[a], Kun Liu[b]

[a] Centre for Autonomous Marine Operations and Systems (AMOS), Department of Marine Technology, Norwegian University of Science and Technology (NTNU), Norway
[b] School of Naval Architecture and Ocean Engineering, Jiangsu University of Science and Technology, Zhenjiang, China
[c] Department of Mechanical and Structural Engineering and Materials Science, University of Stavanger, Stavanger 4036, Norway

ARTICLE INFO

Keywords:
Ship collision
Bridge girder design
Impact response

ABSTRACT

A key aspect in the design of mega bridge structures across navigable waterways is to ensure bridge safety with respect to accidental ship collisions. Special attention has been paid to providing sufficient impact resistance for bridge sub-structures including piers and pylons. However, the collision design of bridge super-structures such as bridge girders is commonly neglected. In this paper, high-fidelity finite element models of a ship bow and a bridge girder are established. Numerical simulations are conducted to study the structural response of the bridge girder subjected to impact from the ship forecastle. Based on the simulation results, design considerations of bridge girders against ship forecastle collision loads are discussed. The effects of the impact location and relative structural strength are also investigated. A simple but effective strengthening method is proposed to increase the collision resistance of steel bridge girders.

1. Introduction

Accidental ship collision is an important consideration in designing bridge structures across navigable waterways. The high kinetic energy of passing ships pose a serious threat to bridge structures. Therefore, it is important to perform advanced analyses to assess the ability of the bridge structures to resist ship collision loads. For bridge structures across large rivers and fjords, the collision design tends to be more critical because ships that operate in these waterways normally have a greater speed and displacement (i.e., the weight of the ship and the cargo). Therefore, bridges should be designed with adequate ability to resist such ship collision loads without excessive structural damage or collapse.

Pioneering studies on the ship-ship collision were conducted by Minorsky [1]. Based on experiments, empirical force-deformation relationships and energy absorption curves were developed. Later, Pedersen et al. [2] and Amdahl and Eberg [3] investigated the ship-ship collision and ship collision with offshore structures. Several widely used codes such as AASHTO [4] and Eurocode [5] for bridges and NORSOK [6] for offshore structures contain simplified formulae to estimate the ship collision loads. More recently, nonlinear finite element (FE) codes such as LS-DYNA [7–10] and ABAQUS [11,12] have been widely used for ship collision analysis. These works have offered good insights into the structural behavior during ship collisions. However, most studies focused on the ship-ship collision and ship collision with offshore structures. For the ship-bridge collision, the available literature is limited. Yuan and Harik [13,14], Consolazio et al. [15–18], Sha and Hao [19–21] and Wang and Morgenthal [22,23] investigated barge collisions with bridge piers. The vessel model in these analyses was typically barges, which have lower and shorter bows than the seagoing ships. In addition, the displacement and travelling speed of barges, and consequently the kinetic energy, are much smaller than those of merchant ships. For ship-bridge collision, Fan et al. [24] estimated the collision demand using a simplified interaction model, and an approach to determine the dynamic ship-impact load based on the ship bow force-deformation relationship was later proposed [25]. The equations to estimate the load duration and time history of ship deformation were analytically derived.

In the ship-bridge collision analysis, bridge structures are commonly modeled using rigid bodies [14,15,19]. This technique can largely reduce the modeling effort and computational time while yielding an acceptable prediction of the impact force. However, the impact duration and energy absorption may not be accurately estimated [19]. In addition, the premise of the rigid bridge assumption is that the bridge structure should have a much higher strength than the striking ship. For large-scale solid bridge foundations and piers, this idealization may be reasonable. However, the strength of a bridge girder is not necessarily much larger than that of a ship forecastle. Therefore, the validity of the

* Corresponding author at: Centre for Autonomous Marine Operations and Systems (AMOS), Department of Marine Technology, Norwegian University of Science and Technology (NTNU), Norway.
E-mail addresses: yanyan.sha@ntnu.no, yanyan.sha@uis.no (Y. Sha).

https://doi.org/10.1016/j.engstruct.2019.109277
Received 3 September 2018; Received in revised form 30 May 2019; Accepted 5 June 2019
Available online 18 June 2019

rigid bridge assumption should be carefully checked in each case.

All of these works address the response of bridge substructures, i.e., piers, piles and pile caps. There has been virtually no focus on the analysis and design of bridge superstructures against ship collisions [26,27]. Due to the increasing height of modern ships, especially large cruise ships, the possibility of a ship forecastle or deckhouse hitting the bridge girder has significantly increased. Such accidents can be catastrophic for both road users on the bridge and passengers on the ship [28]. For example, The Binh Bridge, a three-span cable-stayed bridge in Vietnam, was collided by a ship deckhouse resulting in serious damage to the bridge girder and stay cables in 2010. Later in 2015, The Friesenbrücke Bridge, a 335 m long railway bridge in Germany, was crushed and destroyed by the bow of a cargo ship "Emsmoon". In fact, bridge girders are primarily designed for permanent loads and live loads in the vertical direction, whereas the transverse ship collision loads are neglected. Thus, there is little experience in estimating the bridge girder response to such loads and the proper design against them.

The analysis of ship collision with long floating bridges comprises two tasks, i.e., assessment of the local damage and global response. It is often convenient to split these tasks into two separate analyses. Local deformation and damage evaluation require detailed finite element models of the bridge component and ship structure with explicit nonlinear finite element programs [29]. The global response for long bridges is simulated using a dynamic time domain analysis that addresses the global deformation and forces in the bridge under the action of the collision forces, [26,30,31]. This paper focuses on the first task, i.e., analysis of the resistance, damage and energy dissipation capability in the local contact area. The global response, which determines the demand for local energy dissipation, is not considered. Finite element models of a cruise ship bow and a section of a floating bridge girder are first developed. The cruise ship bow and bridge girder are representative of an early design for the Bjornefjorden floating bridge concept in Norway [32]. Numerical simulations of the ship forecastle collision with the bridge girder are conducted using the FE code LS-DYNA [33]. The impact force and damage evolution are obtained for the preliminary structural design. Parametric studies are conducted to further investigate the effect of the ship- bridge girder relative strength and collision contact location. A bridge girder strengthening technique against transverse ship collision loads is proposed and verified based on the bridge girder damage pattern.

2. Finite element models

In this section, finite element models of a cruise ship bow and a bridge girder section are developed based on structural drawings. Well-established principles to model and simulate the ship grounding and ship-ship and ship-offshore structure collisions are used. The numerical approach has been validated to, e.g., Ringsberg et al. [34] and Storheim et al. [35].

2.1. Ship bow model

The finite element model of the ship bow is based on an eight-deck cruise ship named "MS Balmoral" (see Fig. 1(a)) which has a total length of 195.8 m and a beam width of 22.7 m. The finite element model was developed to facilitate simulations of high-speed impacts that cause large bow deformations and collisions with the pontoons, columns and bridge girders; hence, 30.7 m of the whole cruise ship bow was included as shown in Fig. 1(b).

The plate thickness of the ship hull and internal structures was 6–14.5 mm. Because the structures in front of the collision bulkhead are expected to be in direct contact with the bridge girder, this part of the ship is modeled in detail to accurately represent the actual structural strength. As shown in Fig. 2, the shell panels, internal decks, girders, and stiffeners are carefully modeled using the four-node Belytschko-Lin-Tsai reduced integration shell elements with a size of approximately 100 mm. For detailed information about the modeling of the ship bow, refer to Sha et al. [26]. The rear of the bow model is sufficiently far from the damage zone that the boundary conditions should have a negligible effect. In the simulations, the rear nodes were assumed to move with a constant forward velocity and were fixed in all other degrees of freedom.

2.2. Bridge girder

A number of floating bridge/tunnel concepts have been proposed for the Coastal Highway Route E39 project as shown in Fig. 3. The floating bridge concept investigated in this work includes two cable-stayed spans and nineteen floating continuous spans is illustrated in Fig. 3(a). The two cable-stayed spans in the south end are supported by a 216.5 m high reinforced concrete tower with 84 cables. The channel between the tower and the first pontoon is designed as the navigation channel for passing ships in the fjord. The north side of the bridge is the continuous spans supported by floating pontoons with a spacing of 197 m. Since the floating bridge is relatively flexible in nature, the bridge girders are designed to have a curvature in the horizontal plane to give extra transverse stiffness. The twin bridge girders are transversely connected by crossbeams. The connections between the supporting columns and bridge girders are integrated structures with bulkheads and frames.

A section of bridge girder in the continues spans was modeled [26] as shown in Fig. 4. The outer plates are 12–14 mm thick. In the longitudinal direction, the shell plating is strengthened by 8- and 10-mm-thick hat stiffeners. In the transverse direction, 600-mm-high and 12-mm-thick diaphragms are installed every 4 m. The flange height and thickness are 250 mm and 12 mm, respectively. Four trusses of the circular hollow section with a diameter of 219 mm and a thickness of 6.3 mm are attached to each diaphragm to provide global shear resistance and maintain the cross-sectional shape. The plates, longitudinal hat stiffeners, and transverse diaphragms of the bridge girder were modeled with four-node shell elements, and the internal trusses were modeled with beam elements, which are rigidly connected to several shell nodes to avoid local overloading. Thus, the details of the force transition between trusses and diaphragms were not considered in this study. In total, 12 sections, i.e., 48 m, of the bridge girder were established. A mesh size of 100 mm, which is similar to that in the ship bow model, was used.

2.3. Material modeling

A power-law hardening material model developed by Alsos et al. [36] was used in this study for steel in both the ship and bridge girder. The material was assumed to be isotropic and modeled using the plane stress J_2 flow theory. The equivalent stress-strain curve is represented by a modified power-law formulation including the plateau strain,

$$\sigma_{eq} = \begin{cases} \sigma_y & \varepsilon_{eq} < \varepsilon_{plat} \\ K(\varepsilon_{eq} + \varepsilon_0)^n & \varepsilon_{eq} \geqslant \varepsilon_{plat} \end{cases}, \tag{1}$$

where K and n are strength index and strain index, respectively. $\sigma_y\sigma_y$ is the initial yield stress. $\varepsilon_{eq}\varepsilon_{\mathrm{plat}}$ is the equivalent plastic strain and ε_{plat} is the equivalent plastic strain at the plateau exit. The strain ε_0 $\varepsilon_0$enables the plateau and power-law expression to intersect at (ε_{eq} $\varepsilon_{\mathrm{plat}}$, $\sigma_y\sigma_y$) and is obtained by

$$\varepsilon_0 = \left(\frac{\sigma_y}{K}\right)^{\frac{1}{n}} - \sigma_{eq}. \tag{2}$$

Material failure was considered by incorporating the Rice-Tracey-Cockcroft-Latham (RTCL) damage criterion [36]. The element size for the FE model is approximately 5–10 times the plate thickness. To better predict the strain-induced fracture, the damage criterion is scaled

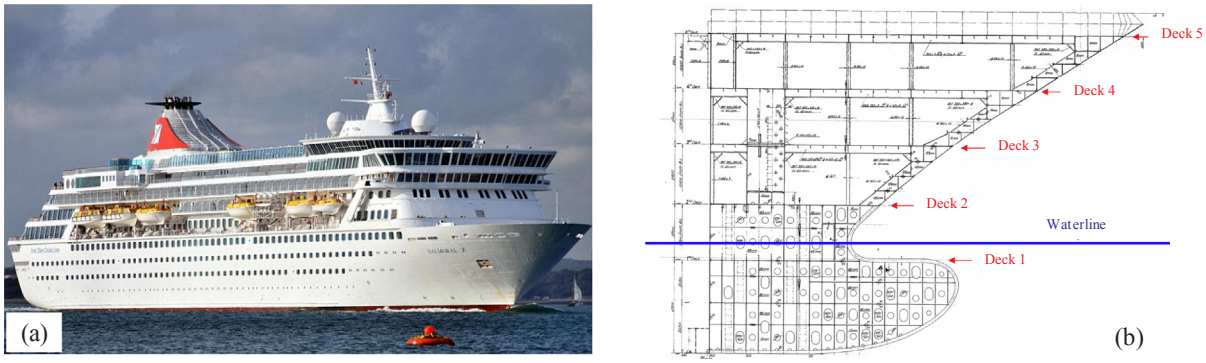

Fig. 1. The design ship MS Balmoral, (a) the real ship and (b) drawing of the ship bow.

according to the mesh size as follows

$$\varepsilon_{cr} = n + (\varepsilon_n - n)\frac{t}{l_e}, \tag{3}$$

where ε_{cr} is the critical strain and ε_n is the failure strain in uniaxial tension for mesh size l_e, which is equal to plate thickness t.

The ship was fabricated in mild steel. The yield stress was set to 275 MPa to more correctly reflect the expected strength. High strength steel with a characteristic yield stress of 540 MPa was used to construct the bridge girder. According to the recommendations by Storheim and Amdahl [37], strain rate effects are neglected because they are uncertain. Detailed parameters for both materials are tabulated in Table 1.

3. Numerical simulations of the ship-bridge girder collision

With the FE models of the ship bow and bridge girder, numerical simulations were conducted to investigate the effect of the relative structural strength and location of impact. The collision force, energy dissipation and structural damage in the bridge girder and ship bow are discussed.

3.1. Forecastle collision with the bridge girder

Bridge girders are designed to resist the vertical dead load from self-weight and live load from passing vehicles. In the transverse direction, the bridge girders are mainly designed for the global reaction induced by the wind load. They are not specially designed to resist transverse impact loads. Hence, the side structures of bridge girders can suffer large deformations and damage if a ship collision occurs. In this section, numerical analyses were conducted to study the bridge girder response to ship collision actions. The ship forecastle was assumed to collide with a bridge girder diaphragm at a constant speed of 10 m/s. This speed would be sufficiently high to reduce CPU consumption for the explicit analysis but sufficiently small to minimize the effect of inertia forces. The ship was only allowed to move in the forward direction, and all of the other five degrees of freedom were fixed at the rear part of the ship bow.

In this study, the relative strength of the ship forecastle and bridge girder was varied by manipulating the material properties. In the integrated analysis, both the ship and bridge girder are deformable, and the actual values of the material properties were used. In the two other cases, either the ship or the bridge girder was assumed to be rigid. The force-displacement curves for the three cases are compared in Fig. 5. Per definition, the displacement signifies the motion of the ship rear end and is equal to the penetration of the ship bow and bridge girder.

In the integrated analysis, the impact force first gradually increases when the contact area between the ship and the bridge girder increases. The ship forecastle only interacts with the top oblique bridge girder plate at this stage. When the displacement is approximately 3 m, the impact force attains a local peak of 15 MN followed by a sudden drop. The reason is that the sharp bridge girder edge penetrates the ship hull and initiates shear failure of the forecastle central girder, as shown in Fig. 6(b). When the ship travels further, the lower part of the forecastle contacts with the bottom oblique bridge girder plate, and the impact force increases again. Then, the curve exhibits peaks and troughs due to gradual engaging and crushing of ship forecastle members. Most of the collision energy is dissipated through the deformation and damage of the ship forecastle. The energy dissipated by the ship and bridge girder is 112.9 MJ and 21.4 MJ, respectively.

When the bridge girder is assumed to be rigid, the force level is close to that in the integrated simulation because the actual bridge girder is stronger than the ship forecastle, so the force level is controlled by the forecastle resistance. The damage level of the forecastle is similar to that of a deformable bridge girder as shown in Figs. 6(a)–(f) and 7(b). The collision energy dissipated by the ship forecastle is 129 MJ, which is close to the total energy dissipated by the ship and bridge girder in the integrated analysis for the same deformation level.

When the bow is rigid, the force level is higher than that in the integrated analysis at the beginning of the contact. In this stage, the

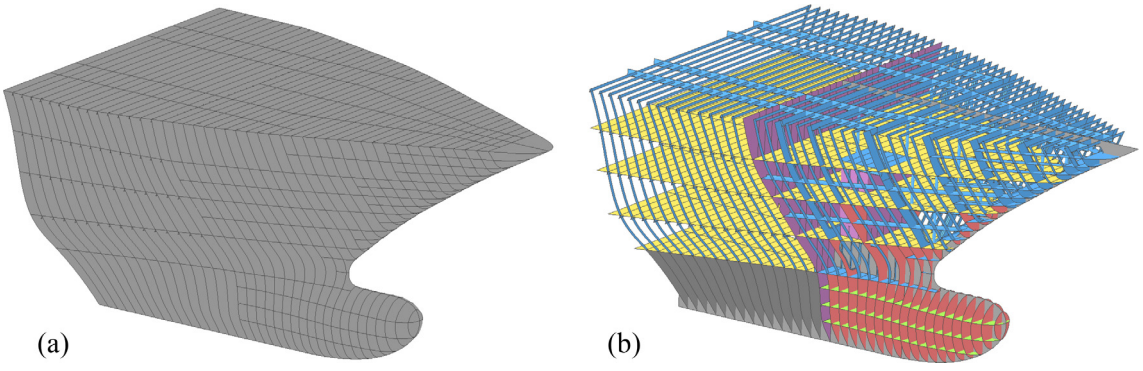

Fig. 2. FE model of the cruise ship bow, (a) outer hull and (b) internal structures.

Fig. 3. Concepts for the fjord-crossing project. (a) Curved floating bridge, (b) tension-leg platform supported floating bridge, and (c) submerged floating tunnel.

bridge girder bending strength controls the force level, whereas the forecastle tip strength governs in the integrated analysis. When the displacement is larger than 2 m, the force is significantly lower due to the fracture of the top bridge girder plate. Then, the bow penetrates the bridge girder with a relatively low force level, and the bridge girder does not benefit from the increasing contact area caused by forecastle crushing. The energy dissipated in the collision is only 61.4 MJ, which is significantly lower than that in the other two cases. Therefore, the assumption of a rigid bow is conservative in terms of the local girder penetration and energy dissipation. However, since the rigid bow assumption yields a relatively low impact force level, it may result in a smaller impact demand in the global response analysis. Consequently, a larger portion of the collision energy has to be dissipated through the global motion of the bridge. Hence, it may be non-conservative to the global capacity of the bridge structure.

In this specific case, the bridge girder is stronger than the ship forecastle and can be considered as being dimensioned according to the "strength design" principle [29], i.e., the girder can resist the total force and corresponding distribution with minor plastic deformations. Therefore, the rigid girder assumption provides a reasonable estimate of the collision force and energy dissipation under the collision of normal strength ship forecastles.

Table 1
Material properties of the ship bow and bridge girder.

	Ship	Bridge girder
Density (ρ)	7850 kg/m^3	7850 kg/m^3
Young's modulus (E)	210 GPa	210 GPa
Poisson's ratio (ν)	0.3	0.3
Yield stress (σ_y)	275 MPa	540 MPa
Strength index (K)	740 MPa	845 MPa
Strain index (n)	0.24	0.12

3.2. Relative strength of the ship and bridge girder

As discussed, the structural response with the assumption of a rigid ship bow or a rigid bridge girder can be quite different. A previous study of ship collision with offshore structures [7] also shows that the relative strength of the striking and struck structures significantly affects the structural deformation and energy dissipation. Therefore, it is necessary to evaluate the sensitivity of the distribution of damage and energy dissipation to the relative strength of the striking ship and struck bridge girder.

Ship bows are designed according to the rules of ship classification societies. For the forecastle, the strength variation of identical size ship bows is moderate, but there are differences. For simplicity and instead of modeling different bows, the parametric study was conducted by

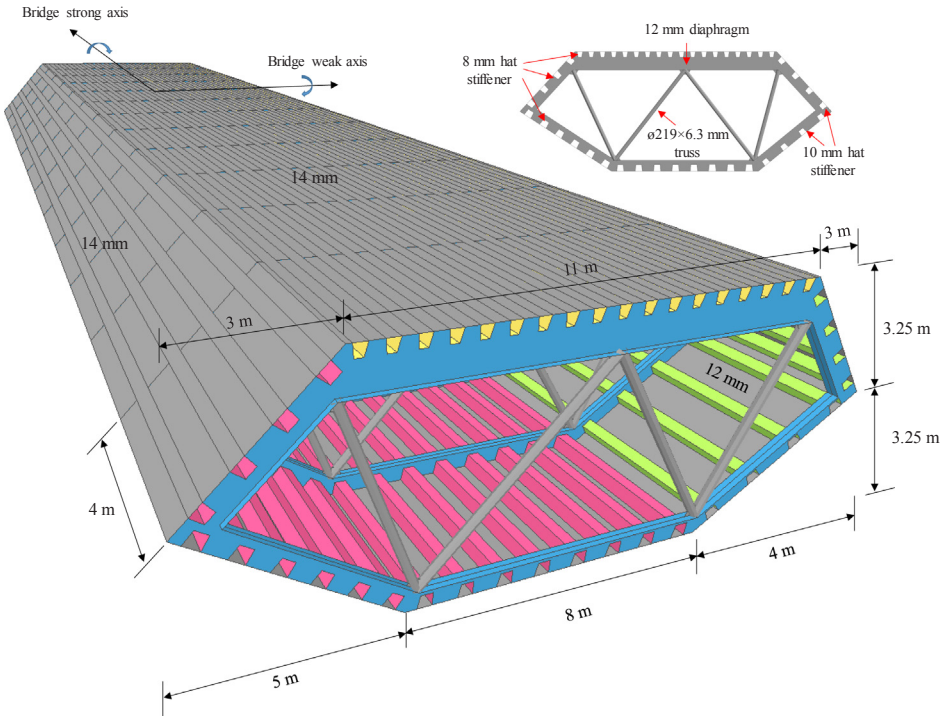

Fig. 4. FE model of the bridge girder, hat stiffeners (red and green), diaphragms (blue), trusses and shell plating (gray). (For interpretation of the references to colour in this figure legend, the reader is referred to the web version of this article.)

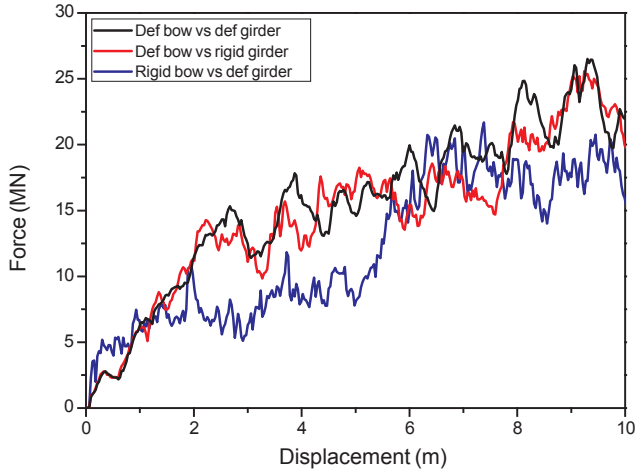

Fig. 5. Force-displacement curves for the impacts of deformable and rigid ship bows with deformable and rigid bridge girders.

varying the grade of the steel material in the ship bow. Three steel grades were used with characteristic yield stresses of 275 MPa, 355 MPa, and 540 MPa and denoted as cases 275OD, 355OD and 540OD, respectively. The first three numbers represent the steel grade, and OD indicates that the ship collides into the bridge girder on the diaphragm. The detailed power law parameters of the three steel grades are listed in Table 2. Collision simulations with various steel grades are also useful because they provide information about the reserve strength ratio (RSR) of the bridge girder with respect to the collision action. The RSR is an often-used concept for offshore structures [38]. The RSR, in this case, may be expressed as the ultimate strength of the bridge girder divided by the resistance generated in the collision with the bow with the nominal yield strength (case 275OD).

Fig. 8(a) displays the force-displacement curves for the three cases. The impact force magnitude is comparable for case 275OD and case 355OD because the bow is weaker than the bridge girder, and the bow strength controls the impact force level. A similar damage pattern is developed, i.e., the bridge girder endures limited deformation while the ship forecastle is cut by the bridge girder (Fig. 8(b)). For case 540OD,

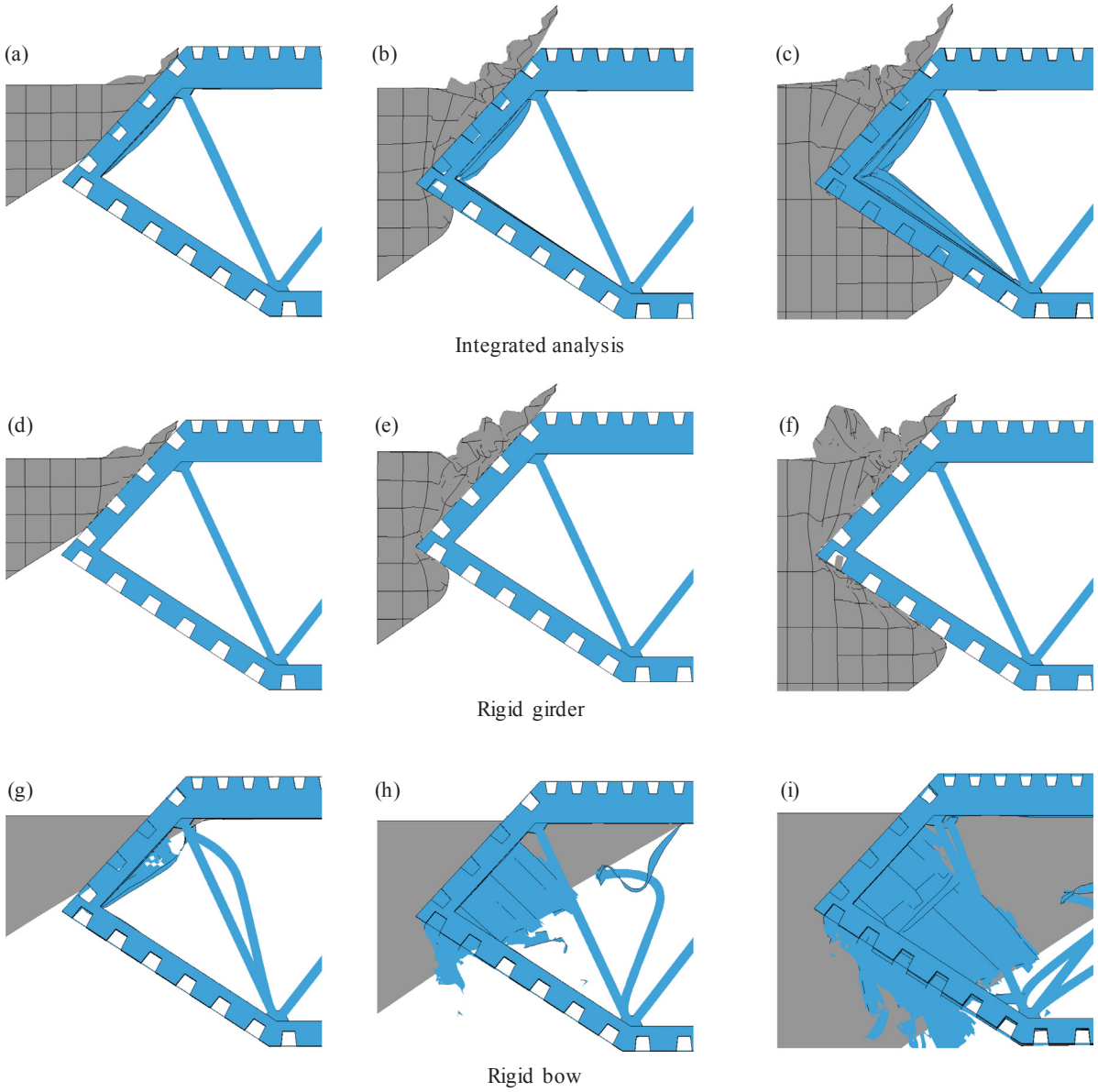

Fig. 6. Side views of structural damage at 1.5 m, 4.5 m and 9 m ship displacement for (a–c) both structures being deformable (integrated analysis); (d–f) deformable bow and rigid bridge girder; and (g–i) rigid bow and deformable bridge girder.

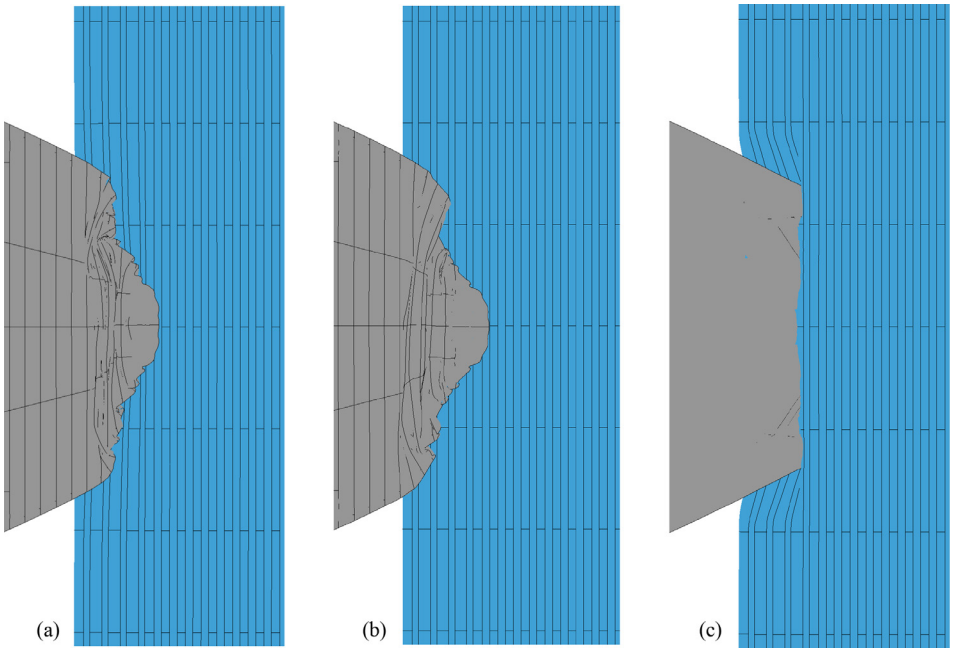

Fig. 7. Top views of the structural damage at 9 m ship displacement for three cases: (a) both structures being deformable (integrated analysis); (b) deformable bow and rigid bridge girder; and (c) rigid bow and deformable bridge girder.

Table 2
Material parameters for the three different steel grades.

	Steel grade 1 (275OD)	Steel grade 2 (355OD)	Steel grade 3 (540OD)
Density (ρ)	7850 kg/m^3	7850 kg/m^3	7850 kg/m^3
Young's modulus (E)	210 GPa	210 GPa	210 GPa
Poisson's ratio (ν)	0.3	0.3	0.3
Yield stress (σ_y)	275 MPa	355 MPa	540 MPa
Strength index (K)	740 MPa	760 MPa	845 MPa
Strain index (n)	0.24	0.19	0.12

the impact force is initially larger than the two other cases because the ship is stronger than the bridge girder in this case. The bending deformation of the bridge girder plate results in a larger contact area and an even larger contact force. A steep drop is observed when the ship displacement is 2.2–3 m because large strains initiate the rupture of the oblique plate on top of the bridge girder. Then, the plate is penetrated by the ship forecastle. The force level is much lower when the crushing depth is 4–6 m because there is less interaction between the ship and the bridge girder.

The difference is more evident in the energy dissipation curves in Fig. 8(b). The ship dissipates approximately 85% of the total collision energy in case 275OD and case 355OD. The bridge girder endures only limited structural damage, so the strength of the ship bow dominates the force level. For case 540OD, the ship is stronger than the bridge girder, and the distribution is reversed. The bridge girder endures excessive damage, whereas limited deformation occurs in the ship forecastle. Only 20% of the total collision energy is dissipated by the ship.

Fig. 9 shows that the structural damage is also strongly related to the relative strength of the ship forecastle and bridge girder. For ships

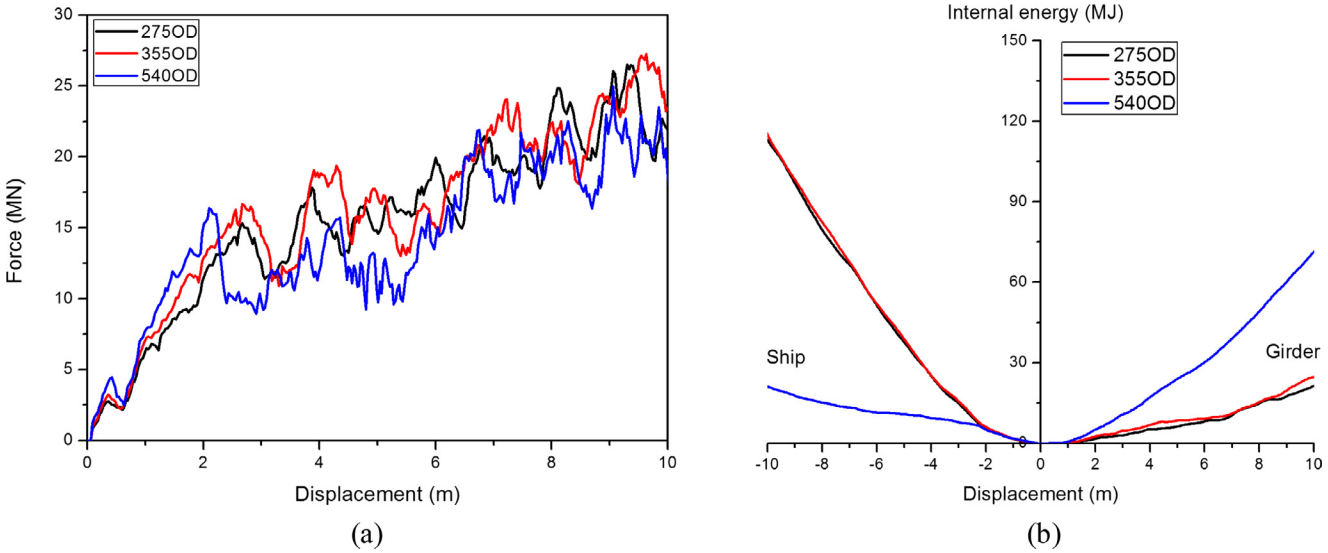

Fig. 8. (a) Force-displacement curves and (b) energy dissipation curves for high position contact on the diaphragm for ship bow steel grades of 275 MPa, 355 MPa and 540 MPa.

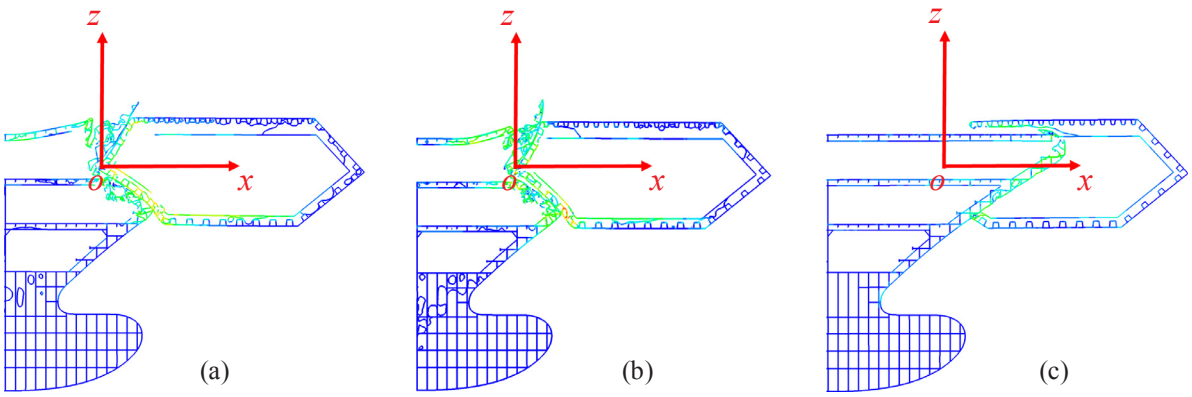

Fig. 9. Damage patterns of the ship bow and bridge girder for (a) case 275OD, (b) case 355OD and (c) case 540OD.

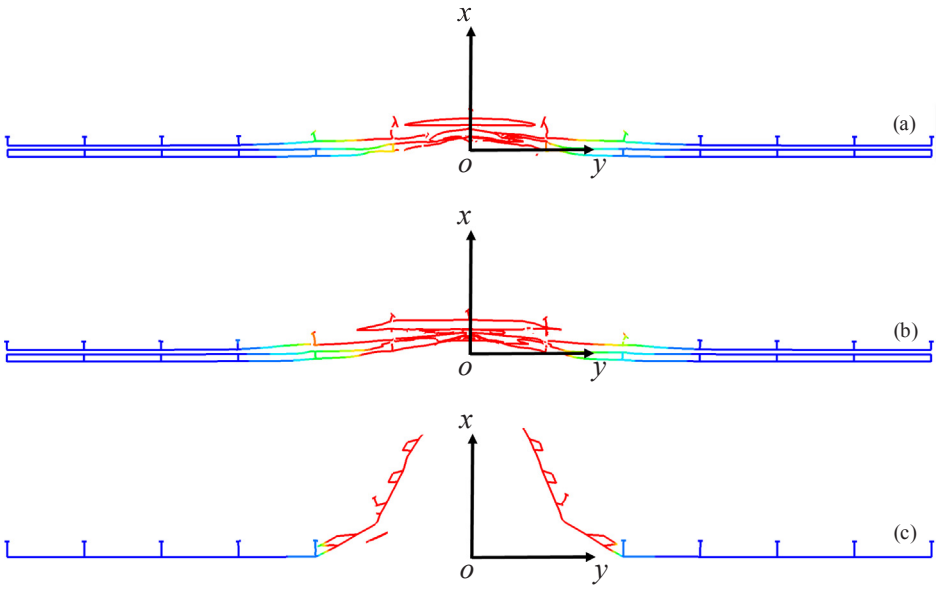

Fig. 10. Top view of the bridge girder deformation at zero origin in Fig. 9 for (a) case 275OD, (b) case 355OD and (c) case 540OD where the bridge girder is subjected to complete penetration.

constructed with higher steel grade, i.e., 540 MPa in this case, the ship cuts the bridge girder plates and deeply penetrates into the bridge girder. This phenomenon is also illustrated in Fig. 9(c) with a horizontal cut through the bridge girder. Fig. 10(a) and (b) demonstrate that when the ship is weaker than the bridge girder, the contact area and bridge girder deformation increase with increasing steel grade. The bridge girder experiences limited local damage and can maintain its functionality.

3.3. Impact location

The ship may hit the bridge girder in an arbitrary horizontal position, and the vertical location may also vary depending on the tide, ship draught and pitch/heave motion. The damage predicted for the three potential locations in Fig. 11 is compared in this section. In the horizontal plane, the ship is assumed to directly collide onto the bridge girder both on one of the diaphragms (case 275OD) and between two adjacent diaphragms (case 275BD). Vertically, the ship collides with the top (case 275OD) and bottom (case 275ODL) oblique bridge girder plates.

Given the bridge girder is generally stronger than the forecastle, the force-displacement curves are notably similar for cases 275OD and 275BD regardless of the relative horizontal impact location as shown in Fig. 12. However, the bridge girder dissipates slightly more energy when the ship collides between two diaphragms as shown in Fig. 12(b).

With further inspection of the bridge girder deformations in Fig. 13, the difference in energy dissipation can be related to the local damage pattern for the two impact locations.

For case 275OD, the impacted diaphragm buckles early at 3 m ship displacement, which causes a drop in the force-displacement curve in Fig. 14(a). The diaphragm failure activates the plate membrane resistance in the longitudinal direction. Two sections of the bridge girder structure mainly contribute to the resistance.

For case 275BD, only one section of the bridge girder engages in the collision in the early stage. The longitudinal stiffeners and bridge girder plates in the section deform by the combined effect of shear and bending. Plate failure occurs at the two adjacent diaphragms, and more severe bending is observed in the stiffeners. When the ship crushes further, three sections of the bridge girder structures become involved. The failure of the longitudinal stiffeners and global bending about the vertical axis become significant.

In general, the impact force is not sensitive to the horizontal location of the contact point. The bow resistance controls the overall force level. However, locally at the impact location, the bridge girder damage is different. A collision between two diaphragms, which is more likely to occur, causes the shear failure of the plate and stiffener at the location of the adjacent diaphragms, as shown in Fig. 13. The structural deformation and energy dissipation in the bridge girder will also be

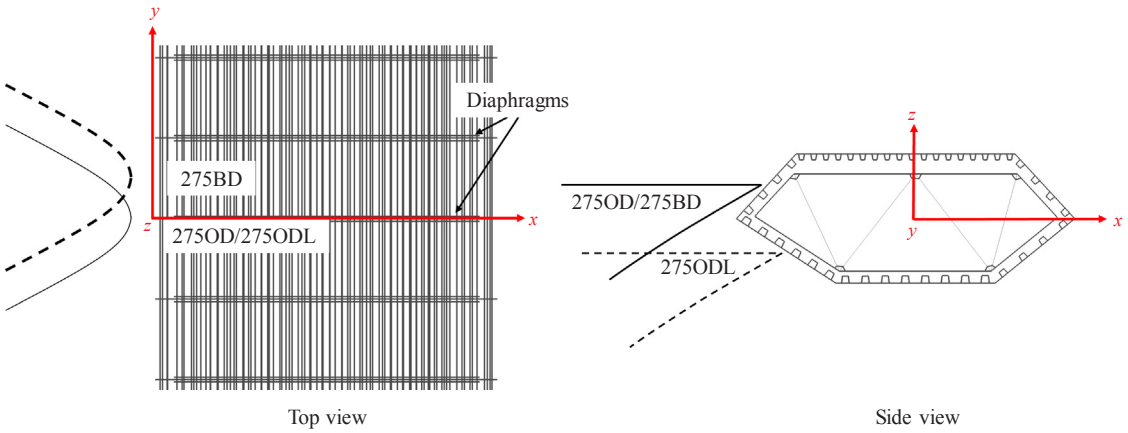

Fig. 11. Illustrations of different horizontal and vertical collision locations of the ship forecastle versus the bridge girder.

more significant.

The effect of the vertical impact location can be significant because it controls the contact area. Naturally, a higher vertical position corresponds to a larger contact area and a larger force (see Fig. 14). Thus, the ship endures greater damage and absorbs more energy in case 275OD than in case 275ODL.

A clear difference in the damage pattern is also observed in Fig. 15. For case 275OD, the ship directly crushes into the bridge girder, and significant interaction occurs between the ship and the bridge girder. For case 275ODL, large deformation occurs in the ship forecastle from the beginning. Then, the ship tends to have a "sliding contact" with the bottom plates of the bridge girder. Simultaneously, the bridge girder is subjected to a lift force from the forecastle. This vertical force induces a torsional moment in the bridge girder, which should be further checked in the design process [26]. The vertical component of the impact force is also shown in Fig. 14(a).

3.4. Girder boundary condition

For the bridge girder, both ends of the bridge girder were fixed in all translational and rotational degrees during the collision simulation. Given the size of the model is relatively large compared to the local contact area, the boundary condition should have a relatively small effect on the local resistance to penetration, possibly with the exception of some overestimation of the resistance contribution from longitudinal membrane forces at very large deformations. Nevertheless, a numerical study was conducted to validate the fixed boundary assumption. An extended bridge girder model of 197 m (between two supporting pontoons) was established including the detailed bridge section and the adjacent bridge girders and crossbeam. The extended part was modelled by resultant beam elements to correctly reflect the cross-sectional properties of the bridge girder and the crossbeam. The extended model is shown in Fig. 16.

The collision response of the extended bridge girder model and the shell-only bridge girder section model is compared in Fig. 17. In both cases, the ship bow is assumed to impact with the bridge girder between two diaphragms at a high impact location (same impact location as case 275 BD). It is observed that the impact force time history obtained from the shell-only model is almost identical to that from the extended model. The girder damage is also comparable for the two models as shown in Fig. 17(b). Hence, it is concluded that the shell-only bridge girder section model utilized in this study with fixed boundary conditions is reasonable.

4. Bridge girder strengthening against collision

Based on the observed failure mechanism during the ship forecastle-bridge girder collision, a simple but effective strengthening method is proposed for the bridge girder against ship forecastle collisions.

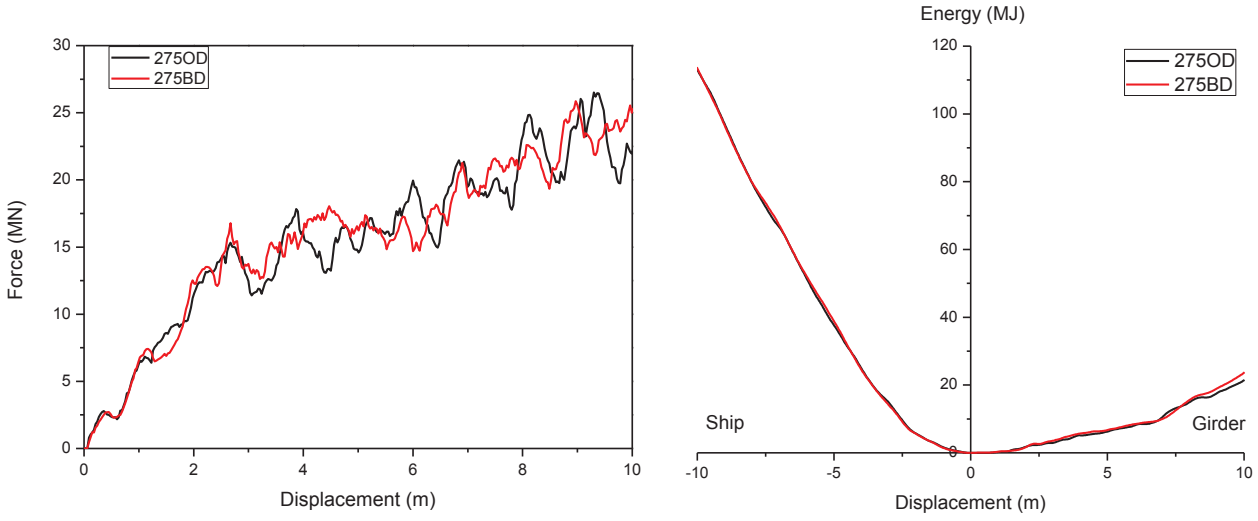

Fig. 12. Effect of the horizontal impact location for high bow position on the diaphragm (275 OD) and between diaphragms (275 BD): (a) force-displacement curves; (b) energy dissipation curves.

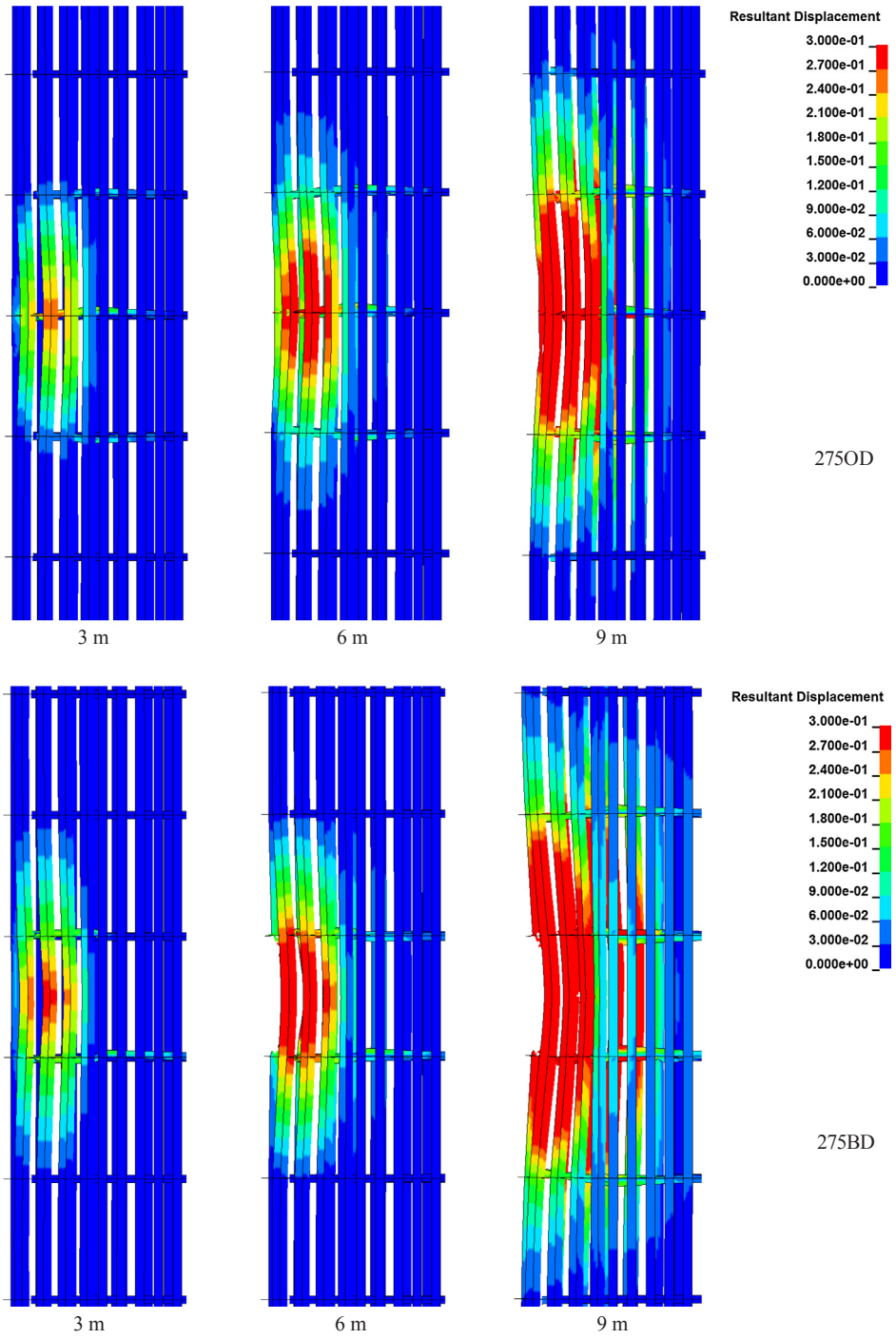

Fig. 13. Bridge girder deformations of 3 m, 6 m and 9 m ship displacements for collision on a diaphragm (275 OD) and between two diaphragms (275BD).

4.1. Bridge girder failure pattern

As discussed, the diaphragm at the impacted area fails by rupture at an early stage, which causes the bending deformation of the top oblique bridge girder plate and quick engagement of two adjacent diaphragms (see Fig. 18). The element begins to erode when the rupture begins, and the degree of rupture is displayed by the eroded internal energy curve in Fig. 19. The eroding energy first occurs in the diaphragm when the ship displacement is only 1.5 m.

A closer inspection of the bridge girder response shows that only the ship forecastle tip contacts with the bridge girder near the top plate at the beginning of the collision. The impact force is very small because it is dominated by the crushing resistance of the forecastle tip. With further crushing, major contact moves downwards. The contact force increased to approximately 10 MN. At this stage, the diaphragm cannot carry the impact load, and shear failure is initiated at the diaphragm end as illustrated in Fig. 20(b).

4.2. Proposed strengthening and validation

Since bridge girders are mainly designed to support the live loads from passing vehicles, a higher diaphragm is only introduced for the diaphragms that support the top bridge girder plate (see Fig. 21). The diaphragms at the bridge girder side are mainly optimized to support the hat stiffeners and transfer the function loads to the bridge girder. They are not designed to resist the local transverse impact loads. To

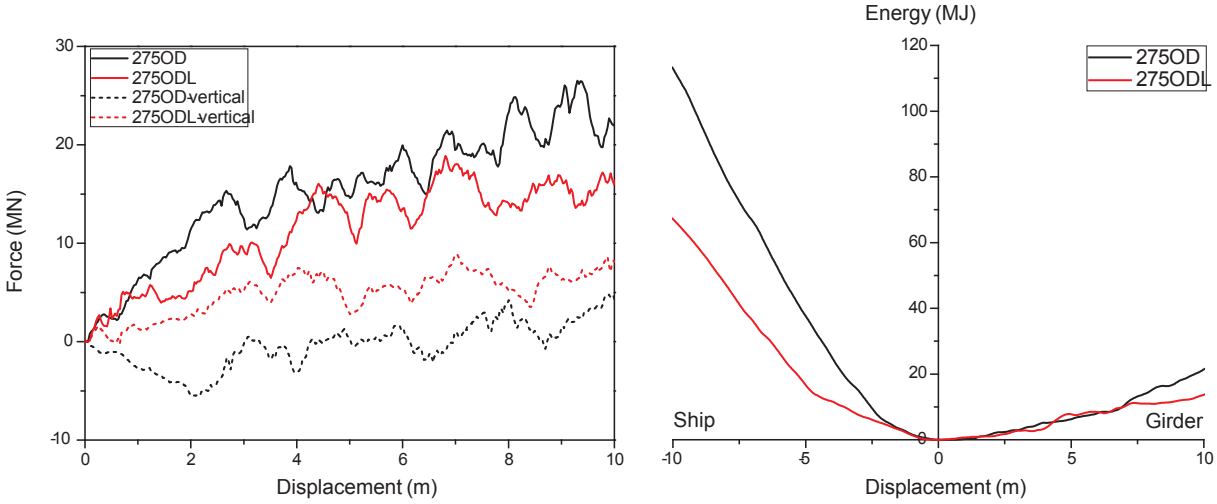

Fig. 14. Horizontal and vertical forces for impact on the diaphragms at a high position (275OD) and a low position (275ODL): (a) force-displacement curves; (b) energy dissipation.

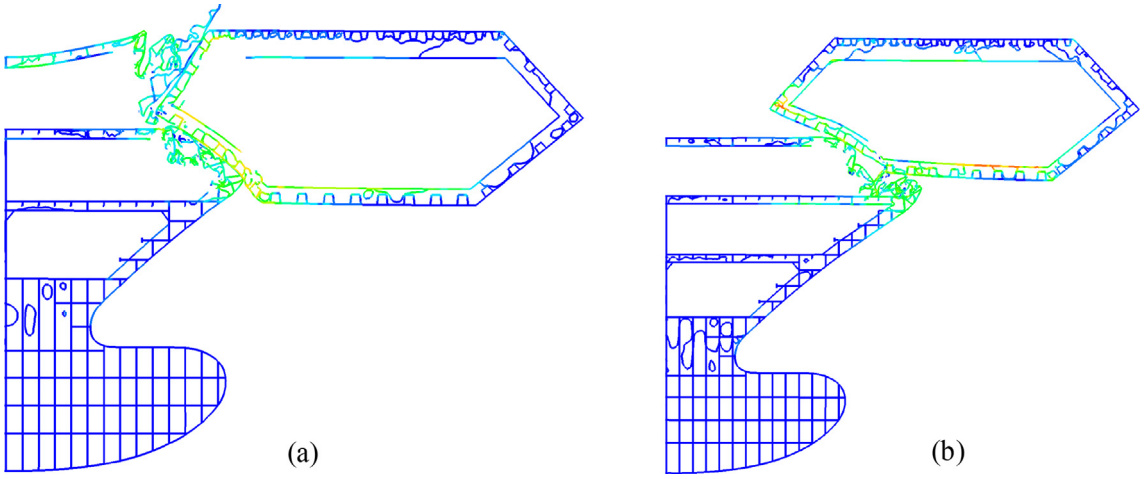

Fig. 15. Damage patterns for two vertical impact locations: (a) case 275OD; (b) case 275ODL.

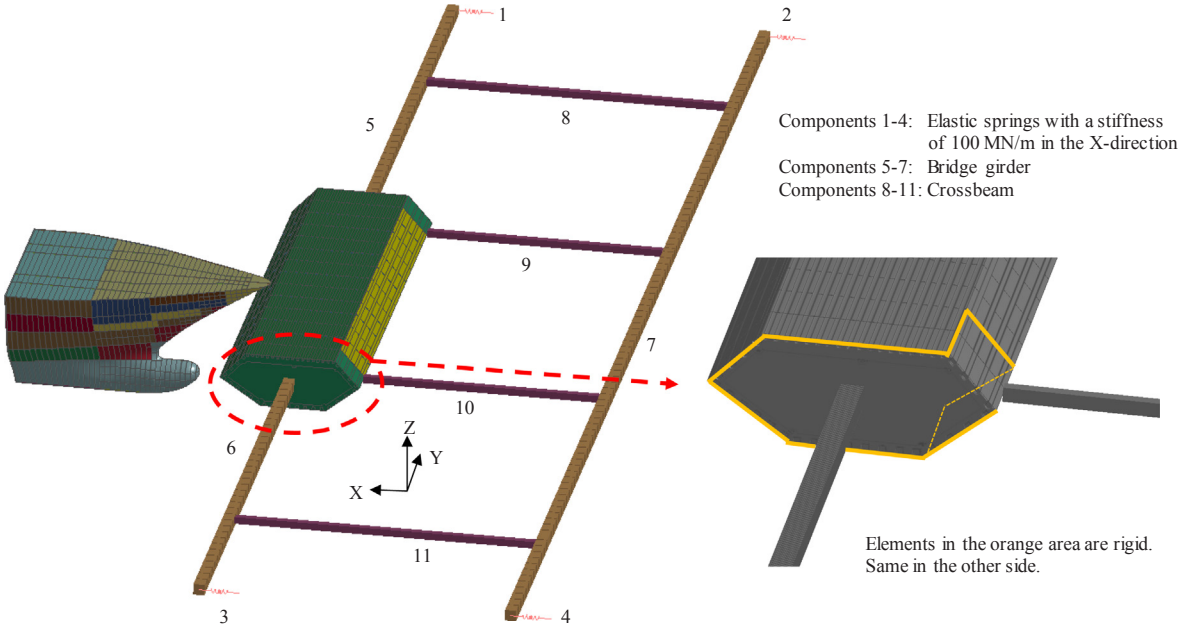

Fig. 16. Extended bridge girder model with beam elements.

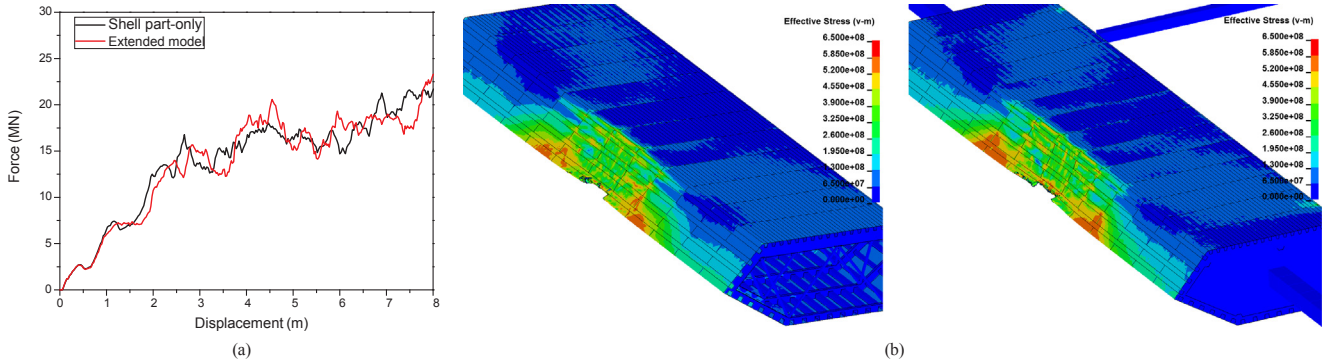

Fig. 17. Comparison of the shell part-only model and the extended model (a) force-displacement curve and (b) girder damage at 8 m ship displacement.

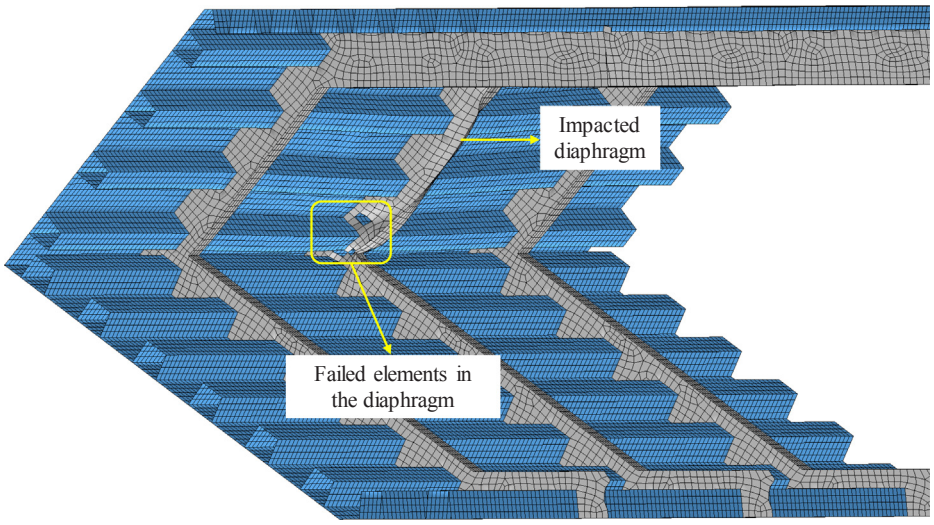

Fig. 18. Internal view of the bridge girder damage for the ship forecastle collision on a diaphragm at a high position.

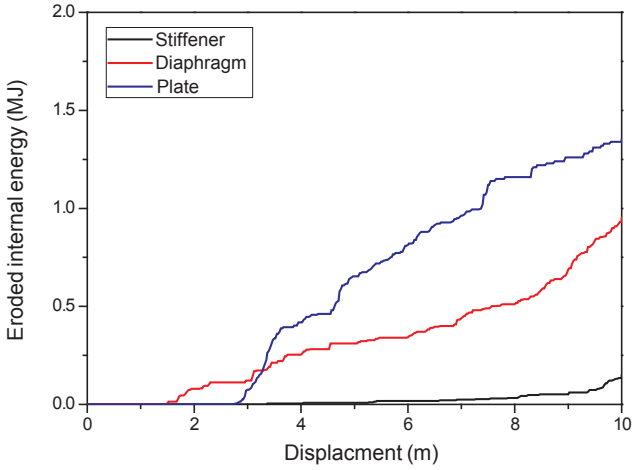

Fig. 19. Curves of the eroded internal energy of various bridge girder components.

increase the resistance to transverse loads, the web thickness or height may be increased. It is considered both technically and economically sound to only increase the diaphragm thickness at the tip end (red area) in Fig. 21.

To demonstrate the effectiveness of the proposed strengthening, a collision case was simulated and compared with the initial unstrengthened design. In this simulation, the thickness of the far end was doubled, i.e., it increased from 12 mm to 24 mm.

The structural response of the strengthened and unstrengthened diaphragms is illustrated in Fig. 22. Upon contact, the diaphragm can resist the shear force in the contact area, and the shear stress level is comparable for the two cases. At a later stage, a clear difference is observed. The unstrengthened diaphragm suffers from shear failure at the lower end. The strengthened diaphragm remains intact at the same force level and transfers more forces to the lower side shell of the diaphragm. No element failure or erosion occurs, and the bending deformation of the upper side diaphragm is greatly reduced as shown in Fig. 22.

The bridge girder deformations with and without strengthening at the end of the collision (10 m ship displacement) are compared in Fig. 23. In the unstrengthened case, large shear stresses in the diaphragms, which ultimately lead to fracture and element erosion, are observed. In the strengthened case, the diaphragm remains generally intact with very limited deformation. The bending deformation of the bridge girder grillage is also significantly reduced. Therefore, a significant improvement of the collision resistance is achieved for the strengthened bridge girder in this special case.

The curves of eroded internal energy are shown in Fig. 24(a). The bridge girder of the original design (case 275OD) has an early initiation of damage when the ship displacement is only 1.47 m. For the strengthened design (case 275ODS), the diaphragm remains intact until the ship displacement is 7.77 m as shown in Fig. 24(a). The eroded energy in the diaphragm is less than 0.1% of the total energy dissipation at the end of the collision.

The overall energy dissipation curves of the ship and bridge girder in the strengthened and unstrengthened cases are compared in Fig. 24(b). The ship forecastle absorbs similar energies in both cases,

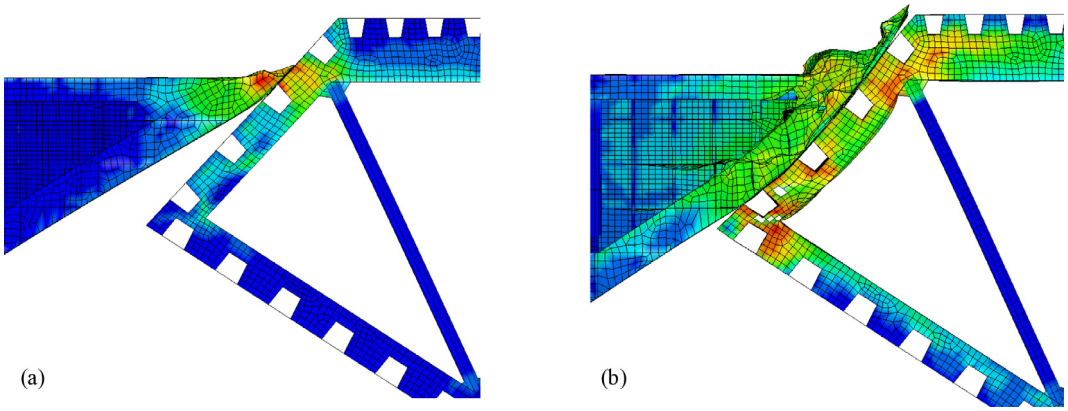

Fig. 20. Bow and bridge girder damage (a) upon contact and (b) when the diaphragm failure begins.

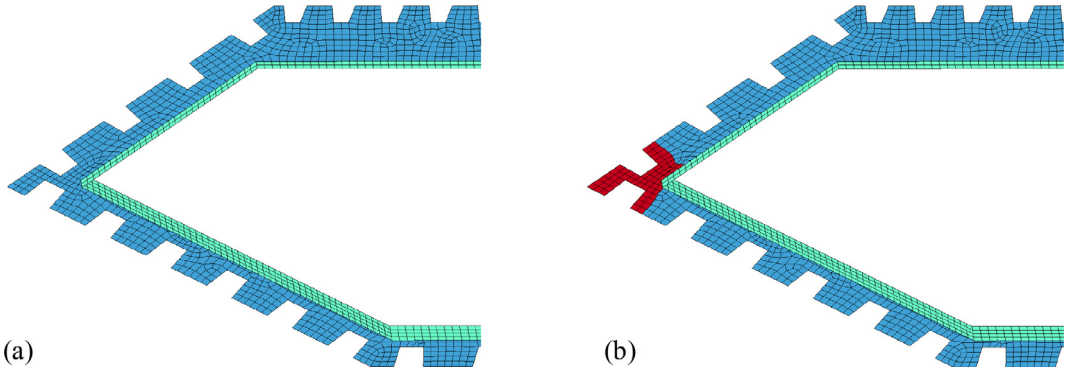

Fig. 21. (a) Initial bridge girder design and (b) strengthened diaphragm end with double thickness.

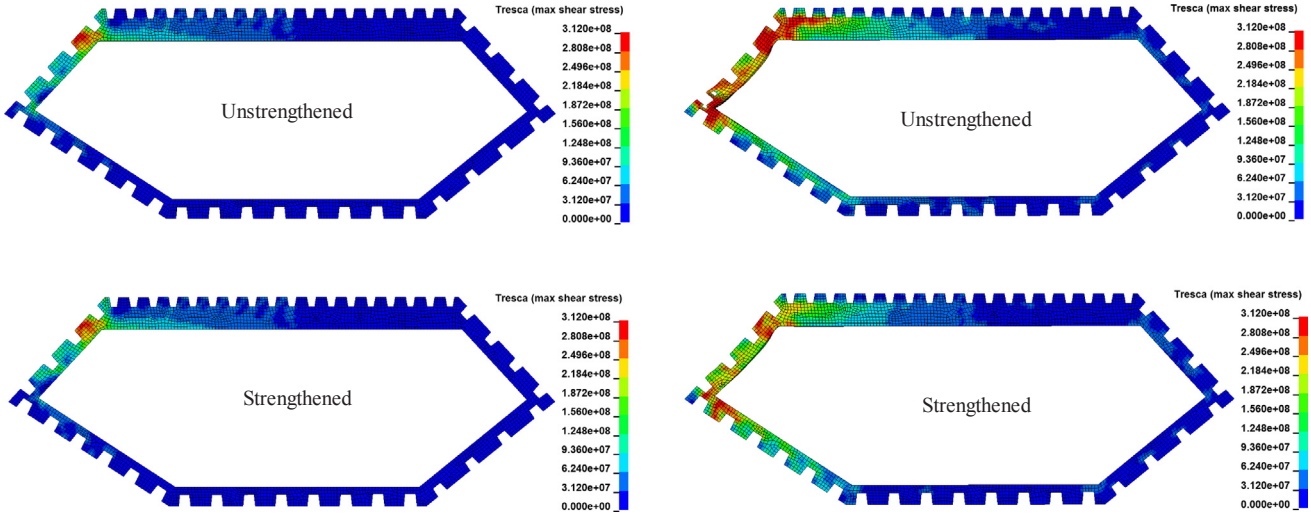

Fig. 22. Maximum shear stress [Pa] for the unstrengthened and strengthened diaphragms at two different ship displacement levels. High bow position contact on the diaphragm.

and the strengthened case has slightly higher energy absorption. The bridge girder with the strengthened diaphragm dissipates only 6.7 MJ collision energy compared to 21.4 MJ in the unstrengthened case. Hence, this notably moderate strengthening effectively reduces the bridge girder damage by 69%, which is substantial.

The collision forces before and after strengthening are compared in Fig. 25. The impact force level is comparable with and without strengthening in the early stage. After 6 m of crushing depth, the collision force in the strengthened case is slightly smaller because the bridge girder plates deform more in the unstrengthened case, which results in a “wrapping effect” and consequently a larger contact area.

Therefore, the proposed strengthening improves the impact resistance of the bridge girder with a notably limited increase in cost and construction effort. The proposed technique may also be conveniently applied to strengthen existing bridge girders.

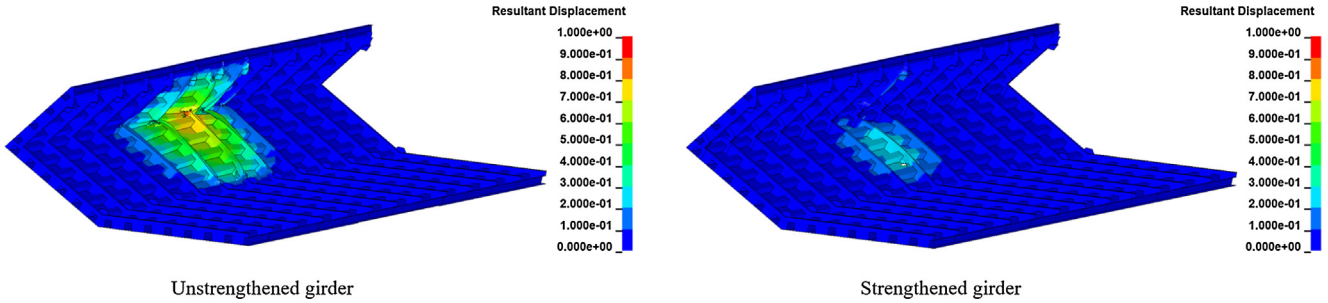

Fig. 23. Deformed configuration of the unstrengthened bridge girder and strengthened bridge girder at the end of the collision. High bow position contact on the diaphragm.

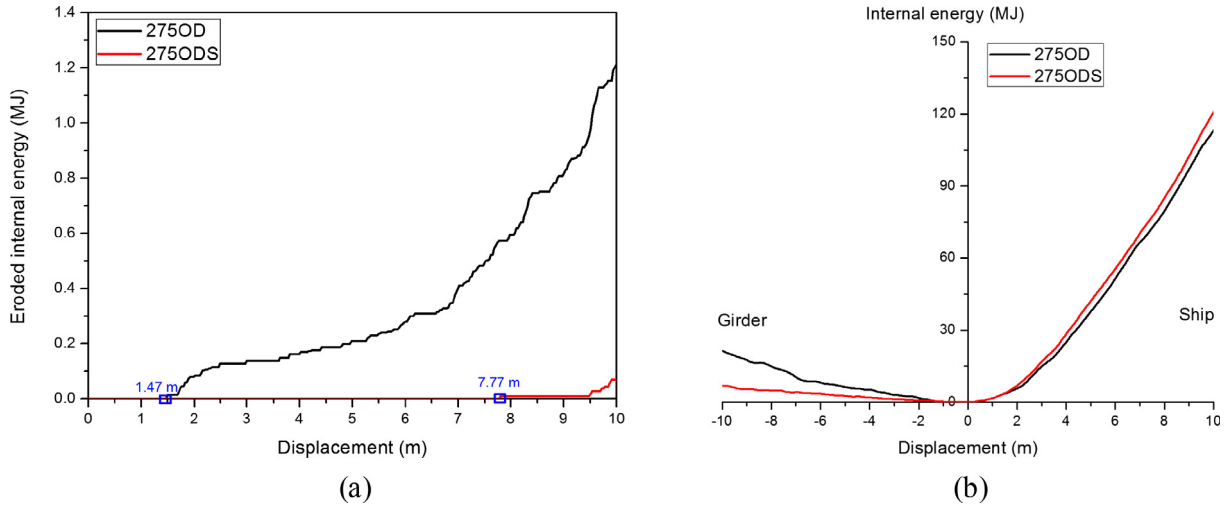

Fig. 24. Comparison of the (a) eroded internal energy of the diaphragm and (b) energy dissipation of the ship and bridge girder for unstrengthened (275OD) and strengthened cases (275ODS). High bow position contact on the diaphragm.

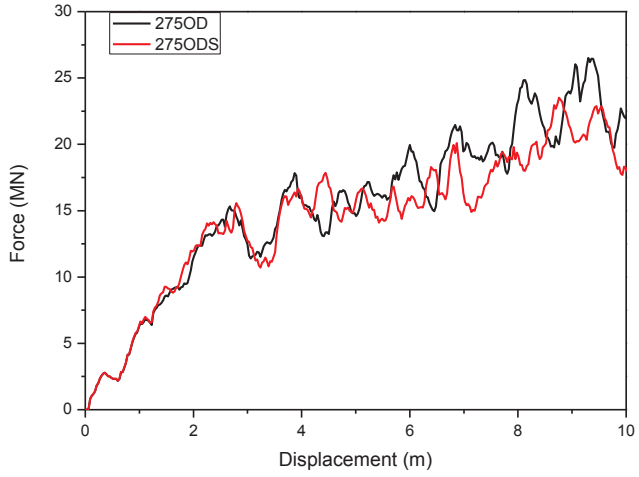

Fig. 25. Force-displacement curves of the initial design (275OD) and strengthened bridge girder (275ODS).

5. Conclusions

Collison between the forecastle deck of a cruise ship and a steel bridge girder was investigated using numerical analysis with high-fidelity models of both structures. The energy dissipation capability by local deformations was the focus, whereas the demand for energy dissipation based on the global response of the bridge was not assessed. The following conclusions are made:

1. The resistance of the ship forecastle was generally smaller than the resistance of the bridge girder. The ship forecastle was torn open and subjected to significant crushing, whereas the bridge girder suffered minor deformation. The collision force was largely governed by the forecastle crushing resistance and essentially identical to that obtained with a rigid bridge girder.
2. To reveal the significance of the relative resistance of the forecastle deck and bridge girder, the yield strength of the forecastle deck was artificially magnified from mild steel (yield stress: 275 MPa) to a higher steel grade with a yield stress of 355 MPa. The response was similar, which indicates that there was a significant strength margin in favor of the bridge girder. When the yield strength was 540 MPa, the relative strength switched in favor of the forecastle. The forecastle was sufficiently strong to tear open the bridge girder and further penetrate it with relatively low resistance.
3. The collision force was relatively independent of the horizontal impact location because the lower ship forecastle strength governed the collision force. The local bridge girder damage slightly depended on the impact locations. For collisions between two diaphragms, shear failure at the two supporting diaphragms was more critical.
4. The effect of the vertical impact location was significant because it is directly related to the contact area. A higher contact position caused a larger impact force and severer structural damage to the bridge girder. The damage was smaller for the positions near the bottom plate, but the vertical lifting force to the girder was significant. This result can affect girder integrity and should be further investigated.
5. Shear failure at the diaphragm reduced the overall bending capacity of the girder. A “double-thickness diaphragm end” strengthening technique was proposed to increase the shear capacity of the diaphragm. This simple approach effectively increased the transverse

impact resistance of the girder at a notably limited increase in cost and construction effort. It can also be easily applied to strengthen existing bridge girders.

The described behavior is relevant for the specific design of the bridge girder and ship forecastle deck. Care should be exercised in generalizing this observation; other bridge configurations and ship bow designs may have different relative strengths.

Acknowledgements

This work was supported by the Norwegian Public Roads Administration (project number 328002) and in part by the Research Council of Norway through the Centres of Excellence funding scheme, project AMOS (project number 223254). The support is gratefully acknowledged by the authors.

Appendix A. Supplementary material

Supplementary data to this article can be found online at https://doi.org/10.1016/j.engstruct.2019.109277.

References

[1] Minorsky V. An analysis of ship collisions with reference to protection of nuclear power plants. New York: Sharp (George G.) Inc.; 1958.
[2] Pedersen PT, Valsgaard S, Olsen D, Spangenberg S. Ship impacts: bow collisions. Int J Impact Eng 1993;13:163–87.
[3] Amdahl J, Eberg E. Ship collision with offshore structures. In: Proceedings of the 2nd European Conference on Structural Dynamics (EURODYN'93), Trondheim, Norway, June1993. p. 21–3.
[4] AASHTO. Guide Specification and Commentary for vessel collision design of highway bridges. Washington, DC: American Association of State Highway and Transportation Officials; 1991.
[5] Vrouwenvelder A. Design for ship impact according to Eurocode 1, Part 2.7. Ship Collision Anal 1998:123–34.
[6] Norsok Standard N. 003. Actions and action effects, edition; 2007. p. 2.
[7] Storheim M, Amdahl J. Design of offshore structures against accidental ship collisions. Mar struct 2014;37:135–72.
[8] Travanca J, Hao H. Numerical analysis of steel tubular member response to ship bow impacts. Int J Impact Eng 2014;64:101–21.
[9] Gao Y, Hu Z, Ringsberg JW, Wang J. An elastic–plastic ice material model for ship-iceberg collision simulations. Ocean Eng 2015;102:27–39.
[10] Liu B, Soares CG. Assessment of the strength of double-hull tanker side structures in minor ship collisions. Eng Struct 2016;120:1–12.
[11] Servis D, Samuelides M, Louka T, Voudouris G. Implementation of finite-element codes for the simulation of ship-ship collisions. J. Ship Res. 2002;46:239–47.
[12] Hogström P, Ringsberg JW. Assessment of the crashworthiness of a selection of innovative ship structures. Ocean Eng 2013;59:58–72.
[13] Yuan P, Harik IE. One-dimensional model for multi-barge flotillas impacting bridge piers. Comput-Aided Civ Infrastruct Eng 2008;23:437–47.
[14] Yuan P, Harik IE. Equivalent barge and flotilla impact forces on bridge piers. J Bridge Eng 2009;15:523–32.
[15] Consolazio GR, Cowan DR. Nonlinear analysis of barge crush behavior and its relationship to impact resistant bridge design. Comput Struct 2003;81:547–57.
[16] Consolazio GR, Cook RA, McVay MC, Cowan D, Biggs A, Bui L. Barge impact testing of the St. George Island causeway bridge. Department of Civil and Coastal Engineering, University of Florida; 2006.
[17] Getter DJ, Davidson MT, Consolazio GR, Patev RCJES. Determination of hurricane-induced barge impact loads on floodwalls using dynamic finite element analysis. Eng Struct 2015;104:95–106.
[18] Pedersen PT. Review and application of ship collision and grounding analysis procedures. Mar Struct 2010;23:241–62.
[19] Sha Y, Hao H. Nonlinear finite element analysis of barge collision with a single bridge pier. Eng Struct 2012;41:63–76.
[20] Sha Y, Hao H. Laboratory tests and numerical simulations of barge impact on circular reinforced concrete piers. Eng Struct 2013;46:593–605.
[21] Sha Y, Hao H. Laboratory tests and numerical simulations of CFRP strengthened RC pier subjected to barge impact load. Int J Struct Stab Dyn 2015;15:1450037.
[22] Wang W, Morgenthal G. Dynamic analyses of square RC pier column subjected to barge impact using efficient models. Eng Struct 2017;151:20–32.
[23] Wang W, Morgenthal G. Reliability analyses of RC bridge piers subjected to barge impact using efficient models. Eng Struct 2018;166:485–95.
[24] Fan W, Yuan W, Yang Z, Fan Q. Dynamic demand of bridge structure subjected to vessel impact using simplified interaction model. J Bridge Eng 2010;16:117–26.
[25] Fan W, Liu Y, Liu B, Guo W. Dynamic ship-impact load on bridge structures emphasizing shock spectrum approximation. J Bridge Eng 2016;21:04016057.
[26] Sha Y, Amdahl J, Dørum C. Local and global responses of a floating bridge under ship-girder collisions. J Offshore Mech Arct Eng 2018.
[27] Sha Y, Amdahl J. A simplified analytical method for predictions of ship deckhouse collision loads on steel bridge girders. Ships Offshore Struct 2018:1–14.
[28] Xia C, Lei J, Zhang N, Xia H, De Roeck G. Dynamic analysis of a coupled high-speed train and bridge system subjected to collision load. J Sound Vib 2012;331:2334–47.
[29] Norsok N. 004, Design of steel structures. Standards Norway, Rev. 2004; p. 2.
[30] Sha Y, Amdahl J, Aalberg A, Yu Z. Numerical investigations of the dynamic response of a floating bridge under environmental loadings. Ships Offshore Struct 2018;1–14.
[31] Kang L, Magoshi K, Ge H, Nonaka T. Accumulative response of large offshore steel bridge under severe earthquake and ship impact due to earthquake-induced tsunami flow. Eng Struct 2017;134:190–204.
[32] Sha Y, Amdahl J. Numerical investigations of a prestressed pontoon wall subjected to ship collision loads. Ocean Eng 2019;172:234–44.
[33] Hallquist JO. LS-DYNA theory manual 2006;vol. 3:25–31.
[34] Ringsberg JW, Amdahl J, Chen BQ, Cho S-R, Ehlers S, Hu Z, et al. MARSTRUCT benchmark study on nonlinear FE simulation of an experiment of an indenter impact with a ship side-shell structure. Mar Struct 2018;59:142–57.
[35] Storheim M, Alsos HS, Amdahl J. Evaluation of nonlinear material behavior for offshore structures subjected to accidental actions. J Offshore Mech Arctic Eng 2018;140:041401.
[36] Alsos HS, Amdahl J, Hopperstad OS. On the resistance to penetration of stiffened plates, Part II: Numerical analysis. Int J Impact Eng 2009;36:875–87.
[37] Storheim M, Amdahl J. On the sensitivity to work hardening and strain-rate effects in nonlinear FEM analysis of ship collisions. Ships Offshore Struct 2017;12:100–15.
[38] Standardization TIOf. ISO 19902:2007 Petroleum and natural gas industries – Fixed steel offshore structures; 2007.